

Adaptation of RUSLE to Model Erosion Risk in a Watershed with Terrain Heterogeneity

Nadhomi Daniel Luliro¹, John Stephen Tenywa² and Jackson Gilbert Mwanjalolo Majaliwa¹

¹Department of Geography, Geo-Informatics and Climatic Sciences, Makerere University, Kampala, Uganda

²Department of Agricultural Production, Makerere University, Kampala, Uganda

Correspondence should be addressed to Nadhomi Daniel Luliro, danielnadhomi@yahoo.co.uk;
dnadhomi@gmail.com

Publication Date: 28 September 2013

Article Link: <http://scientific.cloud-journals.com/index.php/IJAESE/article/view/Sci-140>



Copyright © 2013 Nadhomi Daniel Luliro, John Stephen Tenywa and Jackson Gilbert Mwanjalolo Majaliwa. This is an open access article distributed under the **Creative Commons Attribution License**, which permits unrestricted use, distribution, and reproduction in any medium, provided the original work is properly cited.

Abstract The modeling capability of the Revised Universal Soil Loss Equation (RUSLE) on a heterogeneous landscape is usually limited due to computational challenges of slope length and slope steepness (LS) factor. RUSLE can be adapted to Arc-Macro (C++) executable programs to obtain LS values even for highly variable landscapes based on Digital Elevation Models (DEMs); and then predict erosion risk. The objective of this study was to compute LS factor from DEM using C++; and predict soil erosion risk in a banana-coffee watershed of the Lake Victoria Basin (LVB) of Uganda. DEM data of Nabajuzi watershed were used as an input file for running the (C++) executable program to obtain LS factor. The predicted LS values were calibrated against tabulated LS values; and a strong linear relationship ($R = 0.998$) was observed between them. The LS factor increased with slope length and slope gradient. Erosion risk across landuse were predicted as follows: small scale farmland ($38 \text{ t ha}^{-1}\text{yr}^{-1}$), built up area ($35 \text{ t ha}^{-1}\text{yr}^{-1}$), grassland ($25 \text{ t ha}^{-1}\text{yr}^{-1}$), woodland ($11 \text{ t ha}^{-1}\text{yr}^{-1}$), shrub land and seasonal wetland ($2.5 \text{ t ha}^{-1}\text{yr}^{-1}$), permanent wetland ($0 \text{ t ha}^{-1}\text{yr}^{-1}$). While across soil units erosion risk was highest on Lixic Ferralsols ($50 \text{ t ha}^{-1}\text{yr}^{-1}$), followed by Acric Ferralsols ($20 \text{ t ha}^{-1}\text{yr}^{-1}$), Arenosols ($15 \text{ t ha}^{-1}\text{yr}^{-1}$), Gleyic Arenosols ($2.5 \text{ t ha}^{-1}\text{yr}^{-1}$), and Planosols ($0 \text{ t ha}^{-1}\text{yr}^{-1}$). The risk of erosion increased linearly with slope gradient in the site ($R = 0.96$). On the steepest slopes (15-18) %, the loss ranged from (38–68) $\text{t ha}^{-1}\text{yr}^{-1}$ and on lowest slopes (0-5) %, the loss was (0–2.5) $\text{t ha}^{-1}\text{yr}^{-1}$. We conclude that embedding C++ with GIS data derives LS factor from DEMs. It provides a bench mark for understanding slope morphology; hence making erosion risk prediction on non-uniform slopes much easier.

Keywords *Erosion Risk, Slope Length and Steepness, Arc-Macro Language, GIS, Watershed*

1. Introduction

Erosion risk is one of the major threats to sustainable agriculture most especially in the tropics [15]. To foster conservation planning, the USLE and its revised structure (RUSLE) are widely used to model erosion risk to scale [13, 34, 36]. Unfortunately, gross criticisms emerge particularly on the part

of slope length and slope steepness (LS) estimation under non-uniform landscapes. The USLE/RUSLE were typically developed for 9% slope gradient and 22.13 m slope length [43]. It is neither suitable for shorter slopes (less than 4 m) [12], nor for longer ones (greater than 120 m) [33]. Whereas several algorithms have been developed to cater for this purpose, none of them is universally acceptable for LS estimation due spatial terrain heterogeneity. There is paucity of information concerning how spatial heterogeneity at watershed scale affects soil erosion processes to foster its monitoring and conservation planning strategies [35]. By and large, the commonest algorithms used in LS estimation include: the grid-based [18]; unit stream power theory [31, 28, 29]; contributing area [6, 7]; neighborhood and quadratic surface, maximum slope and maximum downhill slope [38].

Many of these algorithms, however, are premised on equations such as Equation 1, which assume the exponents to have constant values. Yet, the most realistic approaches for LS computation are those that are anchored on exponential variability with respect to slope gradient [10, 47].

$$LS = [A/22.13]^m \times [\sin \theta/0.0896]^n \quad (\text{Equation 1})$$

Where m and n have constant values of 0.6 and 1.3, respectively; θ is the terrain slope in degrees; A is the upslope contributing area per unit width of cell spacing ($\text{m}^2 \text{m}^{-1}$) from which the water flows into a given grid cell. According to [29], a derived as the sum of all grid cells from which the water flows into the cell expressed as:

$$A = \frac{n\mu a}{b}$$

where a is the area of the grid cell; n is the number of cells draining into the cell; μ is the weight depending on runoff generation mechanism and infiltration rates; and b is the cell spacing.

Adapting RUSLE to a C++ program circumvents LS estimation loopholes [41], hence boosting its modeling capability under terrain heterogeneity conditions. It is postulated that since water flows down slope under gravity, its flow direction can then be North, South, East or West; or Northeast, Southeast, Southwest or Northwest. This method further assumes that if flow converges occur, then the flow direction would be the side of the steepest descent. Considering the pixel grid in the DEM, the C++ program is able to calculate Non-cumulative slope length (NCSL). NCSL is the distance between the centres of the grid cells of the DEM. A cumulative slope length is then computed by summing the NCSL from each grid cell, beginning at a high point and moving down along the direction of steepest descent. This expeditiously computes the LS factor for use in RUSLE from DEMs under conditions that were highlighted by [17] as follows:

- a. If the cell being calculated is a high point then NCSL = 0.5 (cell resolution size);
- b. If the input cell's flow direction is in a cardinal (N,S,E,W) direction then NCSL = (cell resolution size);
- c. Otherwise (flow is in diagonal direction: NE, NW, SE, SW) and NCSL = 1.4142 (cell resolution size).

The objective of this study was to compute the LS factor from DEM based on C++ script; and to predict soil erosion risk in order to identify hot spots for effective conservation planning in a banana-coffee dominated watershed of the Lake Victoria Basin of Uganda.

2. Materials and Methods

2.1. Site Description

The study site was Nabajuzi watershed of the Lake Victoria Basin (LVB) of Uganda, delineated using a hydrological mapping tool (AvSWAT) (Figure 1). This site covers approximately 939 Km². It is traversed by a swampy-bogged stream draining into the River Katonga system that flows into Lake Victoria. The elevation, 1200-1290 m above sea level, of this area is in part attributed to the geologic disturbances that incurred on the old basement complex rocks of the East African plateau. This watershed rests on the old Buganda surface, which is characterized by hills and ridges that were dissected by streams and water ways [16]. From the data gathered from National Agriculture Research Laboratories (NARL) in Kawanda, Uganda, five soil types classified according to the FAO system exist in the site. These soils include: *Acric Ferralsols* (299.49 km²), *Gleyic Arenosols* (147.74 Km²), *Lixic Ferralsols* (463.78 Km²), *Arenosols* (27.72 Km²) and *Planosols* (0.21 Km²). They belong to Buganda, Mirambi, Mawogola and Kabira catenas; and Mulembo, Kifu and Sango series, respectively (Table 1).

Table 1: Soil Classification and Distribution in Nabajuzi Watershed in the Lake Victoria Basin of Uganda

Area (km ²)	Percent (%)	Parent Rock	Mapping Unit	Classification (FAO)	Productivity
230.0	24.5	Toro gneisses and granites	Mawogola catena	Acric ferralsols	Medium to low
44.3	4.7	Recent alluvium	Mulembo series	Gleyic arenosols	Nil to low
178.8	19.0	Toro gneisses and granites	Mirambi catena	Acric ferralsols	High
27.7	3.0	Basement complex gneisses and granites	Katera series	Arenosols	Medium
463.8	49.4	Toro schists and phyllites	Buganda catena	Lixic ferralsols	High
0.21	0.02	Lake deposits	Sango series	Planosols	Nil to low
103.5	11.0	Alluvium and hillwash from basement complex	Kifu series	Gleyic arenosols	Nil to low
Total = 939		100%			

Source: National Agriculture Research Laboratories, Kawanda, Uganda

2.2. Parameterization of RUSLE Factors to Predict Soil Erosion Risk

Erosion modeling was performed based on RUSLE framework [33] as in Equation (2).

$$A = LS^* R^* K^*C^*P \quad (\text{Equation 2})$$

Where, A = Soil loss in t ha⁻¹ over a period selected for R, usually on a yearly basis;

R = Rainfall-runoff erosivity factor in MJ mm ha⁻¹ hr⁻¹yr⁻¹;

K = Soil erodibility factor in t h MJ⁻¹ mm;

L = Slope length factor (dimensionless);

S = Slope steepness factor (dimensionless);

C = Cover and management factor (dimensionless); and

P = Conservation support practices factor (dimensionless).

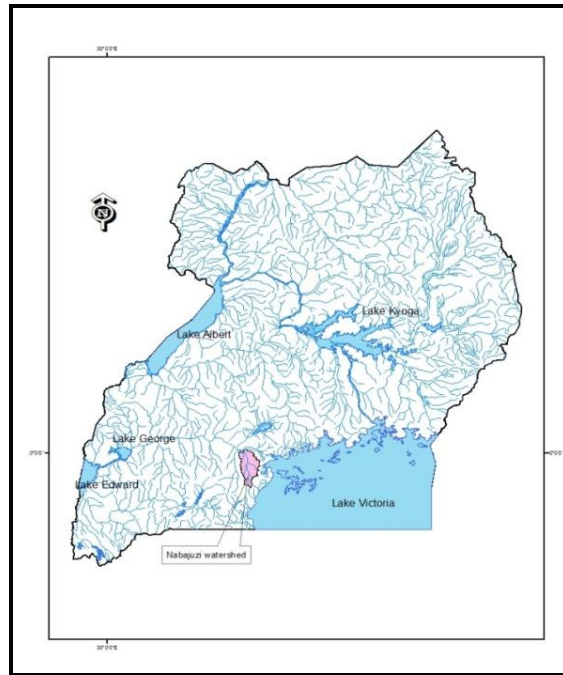


Figure 1: The Drainage Map of Uganda Showing the Location of Nabajuzi Watershed in the LVB

2.3. Procedure for Slope Length and Steepness (*LS*) Estimation

The Arc-Macro Language (AML) method for *LS* calculation was used. It operates in an automatic program, and computes the *LS* values from a DEM to form a single raster layer [41]. This method was first written in an AML [17], but was later updated with the C++ Programming Language to improve its efficiency in data processing. The original AML procedure was hinged on equations that were earlier on developed by [43] for computing slope steepness as:

$$S = (65.41 \times \sin 2\theta) + (4.56 \times \sin \theta) + 0.065 \quad (\text{Equation 3})$$

Where, θ is slope angle in degrees.

However, the upgraded C++ program uses modified slope steepness equations [27] adapted from equation (3) to enable it cater for all terrain variations that could be available in any given watershed. These expressions are presented as in Equation (4).

$$S = 10.8 \times \sin \theta + 0.03, \text{ for slope percent} < 9\%; \text{ and}$$

$$S = 16.8 \times \sin \theta - 0.50, \text{ for slope percent} \geq 9\% \quad (\text{Equation 4})$$

Where θ is slope angle in degrees.

2.4. Computation of *LS* Factor by Adapting RUSLE to C++ Program

The C++ Programming Language was embedded in an ESRI ArcGIS 9.3 environment. A detailed contour map covering the entire watershed was obtained from Ministry of Lands, Housing and Urban Development, Department of Surveys and Mapping, Entebbe, Uganda. A DEM (coded *nabj*) was created by interpolation from Spatial Analysis Tools. This DEM (30 m by 30 m) resolution was used as an input raster file in the C++ Program. Prior to execution, the DEM was first converted to ASCII format using Raster Conversion Tools for easy recognition by the program. After conversion, the C++

executable program was used to run it. In tandem, a series of commands appeared in the command lines in which the path and filename with DEM data (in ASCII format) were entered. The path for the output files was then appropriately defined to enable easy retrieval. The pixel cells with no data in the DEM were ignored in the computation to improve accuracy and precision. Automatically the program filled any depressions or sinks found on the DEM so that the highest elevation points were easily identified. Flow direction was determined by the program; hence enabling the *LS* factor calculation. After execution, sixteen files with suffix (.dat) each containing a different theme (Table 2) were produced. Only *nabjrusle_l.dat*, *nabjrusle_s.dat* and *nabjrusle2.dat* were used because they contained data required for the *LS* factor. The other files such as: *nabjoutflow.dat* and *nabjslp_cut.dat* contained data for the potential deposition areas in this watershed; while *nabslp_exp.dat* contained slope exponents, but this was beyond the scope of this study.

Table 2: A Display of the C++ Program Files after Executing the DEM of Nabajuzi Watershed of LVB of Uganda

					
nabjcell_len.dat	nabjdemfill.dat	nabjinflow.dat	nabjinit_len.dat	nabjlogfile.dat	nabjorig_dem.dat
					
nabjoutflow.dat	nabjrusle_l.dat	nabjrusle_s.dat	nabjrusle2.dat	nabjslp_ang.dat	nabjslp_cut.dat
					
nabjslp_exp.dat	nabjslp_fac.dat	nabjslp_in_ft.dat	nabjslp_len.dat		

The identified *LS* factor files were then converted back to a raster format by adding the suffix (.txt) using the Conversion Tools function in ArcGIS 9.3. The new raster files *nabjrusle_l.txt*; *nabjrusle_s.txt* and *nabjrusle2.txt* were all imported as one layer to form an *LS* factor map of Nabajuzi watershed.

2.5. Procedure for Rainfall Erosivity (*r*) Factor Estimation

The rainfall erosivity factor (*R factor*) is defined as the average annual total of the storm *EI*₃₀ values for a place [33]. *EI*₃₀ is the individual storm index values which equals to *E*, which is the total kinetic energy of a storm, multiplied by *I*₃₀ which is the maximum rainfall intensity in 30 minutes. The multiplication of *EI* reflects the total energy and peak intensity combined in each particular storm. Continuous rainfall records are necessary to calculate the maximum 30 minute rainfall intensity (*EI*₃₀). To obtain an accurate *R factor*, *EI*₃₀ needs to be calculated with continuous records over multiple years for multiple stations located at the area of the study site. The basic equation for determining the *R factor* was earlier developed by [42] as presented in Equation (5).

$$R = \frac{1}{n} * \sum_{j=1}^n [\sum_{k=1}^m (E) * (I_{30})] \quad \text{(Equation 5)}$$

Where: R = Rainfall erosivity factor;

E = Total storm kinetic energy (MJ/ha);

*I*₃₀ = Maximum 30 minute rainfall intensity;

j = Index representing the number of years used to compute the average;

k= Index representing the number of storms in each year;
 n = Number of years to obtain the average; and
 m = Number of storms in each year.

Since total energy (E) and maximum 30-minute intensity (I_{30}) are the rainfall characteristics that are most closely related to the amount of soil erosion produced in an area, the EI_{30} values can be calculated for each rainfall that exceeds 13mm. For this reason, some authors have argued that kinetic energy (E) can be determined from the Equation (6), which was developed by [9].

$$E = 118.9 + 87.3 \log I \quad (\text{Equation 6})$$

Where: E = kinetic energy ($\text{J m}^{-2} \text{mm}^{-1}$); and I = rainfall intensity (mm hr^{-1}).

Alternatively, a modified Fournier index can also be used to estimate the R -factor as used by [20]. Basing on this method, average annual EI_{30} is expressed in $\text{MJ ha}^{-1} \text{mm}^{-1} \text{hr}^{-1}$ is calculated from Equation (7).

$$EI_{30} = 0.3 * \sum(p_i/P)^{1.93} \quad (\text{Equation 7})$$

Where: p_i = mean monthly rainfall (mm); and P = mean annual rainfall (mm).

But criticism has enthralled this index based on the fact that even light rains can cause significant erosion depending on other factors such as soil properties; slope length, steepness, antecedent moisture and vegetation cover [1].

In Vietnam, [14] pointed out that rainfall erosivity indices could simply be determined from mean annual totals as shown in the Equation (8).

$$R = 0.548P - 59.9 \quad (\text{Equation 8})$$

Where: R = rainfall erosivity (J m^{-2}); and P = mean annual rainfall of the area (mm).

While in Indonesia, an earlier study by [3] recommended the use of Equation (9) to determine the rainfall erosivity factor for erosion studies.

$$R = 2.5 * P^2 / [100(0.078P + 0.78)] \quad (\text{Equation 9})$$

Where: R = rainfall erosivity (J m^{-2}); and P = annual rainfall (mm).

In East Africa, standard erosivity indices are usually determined from Equation (10) which was developed by [30].

$$R = 0.029 (3.96P + 3122) - 26 \quad (\text{Equation 10})$$

Where: R = rainfall erosivity (J m^{-2}); and P = the mean annual rainfall of the area (mm).

This index is robust in the sense that it recognizes and computes the erosivity of rainstorms with varying intensities, a salient feature of the torrential rains received in this region. For this reason, this index has been accepted and widely used in different agro-ecological zones of Uganda to estimate rainfall erosivity [24, 25, 2].

2.6. Determining Soil Erodibility (*K*) Factor

Two methods were employed to derive the soil erodibility *K* factor. First, was obtaining soil samples from all the soil units in the site; and establishing the soil erodibility values by nomograph method [43, 33]. This method uses percent silt plus very fine sand (0.002-0.1 mm), percent sand (0.1-2 mm), percent organic matter, and soil structure and permeability classes to calculate the *K* values. Soil structure was interpreted from soil profile descriptions that were made for each soil unit in the site; while permeability codes were assigned to each horizon. Second, was by using the soil layer obtained from National Agricultural Research Laboratories, Kawanda (KARL) and adding soil erodibility values for each soil unit to its attribute table. These erodibility values were computed from the basic Equation (11), which was developed by [43].

$$100K = 2.1M^{1.14}10^{-4}(12 - a) + 3.25(b - 2) + 2.5(c - 3) \quad (\text{Equation 11})$$

Where, *M* = topsoil texture, calculated as (%silt + % silty sand)*(100% - % clay);
a = % of topsoil organic matter content;
b = class of topsoil structure; and
c = class of soil profile permeability.

The corresponding *K* values obtained for each soil unit were added to the table of attributes using the Add Field function in ArcGIS 9.3 to the soil map. This map was then used to generate an erodibility map for the study site.

2.7. Determination of the Crop Cover and Management (*C*) Factor

The *C* factor reflects the effect of cropping and management practices on erosion rates. The *C*-factor could be extracted by an algorithm which combines landuse, canopy cover, surface cover, surface roughness and soil moisture as sub-factors [33]. But some of these parameters may not readily be available for some areas. Thus, circumventing this pitfall, [36] recommended the use of percent canopy- or surface-cover alone to estimate this factor as shown in Equation 12, a method which was adopted for use in the study site in conjunction with image processing.

$$C = 0.6508 - 0.343\log c; \text{ for } 0 < c < 78.3\% \quad (\text{Equation 12})$$

Where: *C* equals 1 and 0, if *c* is equal to 0% and $\geq 78.3\%$, respectively; and *c* is percentage canopy/surface cover.

To generate the *C* factor map, a Landsat Enhanced Thematic Mapper (30 m by 30 m) image of 2010 was acquired and processed using procedures described by [22]. A linear image enhancement technique was performed to increase contrast of features in this image. A pseudo color composite was made with bands 4, 3 and 2, for easy identification of the various land use and land cover types in the watershed. This image was classified using supervised classification procedure using Erdas imagine 9.2. A preliminary land use and cover map was then obtained using the maximum likelihood classifier algorithm. Coupled to this, ground truthing was conducted on-site to synchronize particular land use and cover categories with image classes and the National Biomass data for 2006 (classified according to FAO System), which were obtained from National Forestry Authority (NFA), Nakawa. The *C* factor layer was finally obtained by adding the computed *C* values to the attribute table of the landuse map. These values were obtained based on percent bio-mass for each landuse and land cover class.

2.8. Deriving the Conservation Practice *P* Factor

No erosion physical control structures were identified in the site. The conservation practice factor, *P* was therefore regarded as 1. The layer for this factor was created by re-classifying the DEM image of this watershed. A value 1 was assigned to replace the elevation values for each of DEM grid cells using Spatial Analyst tools, and by selecting the Re-classify Function. The range of values was reset under the column 'old values' from the lowest to highest elevation values of the DEM to make all values of its cells correspond to 1, hence giving rise to a new class which now constitute the *P* factor layer.

3. Results and Discussion

3.1. Calibration of the *LS* Values of Nabajuzi Watershed

The predicted *LS* values obtained from the executed DEM of Nabajuzi watershed using the C++ program was calibrated against tabulated *LS* values for moderate ratio of rill to interrill erosion generated Technical Guide to RUSLE use in Michigan, NRCS-USDA State Office of Michigan [32]. The predicted and tabulated *LS* values were correlated; depicting a strong ($R = 0.998$) linear relationship between them as presented in Figure 2. For shorter slope lengths with low gradients, the predicted and tabulated *LS* values generally conformed to each other. In addition to this, a close association of the said values was also recognized in situations where longer slopes existed at low slope angles. By and large, the predicted *LS* values were utilized as authentic values for use in erosion prediction in Nabajuzi watershed due to the strength of their correction with the tabulated values for rill and interrill erosion.

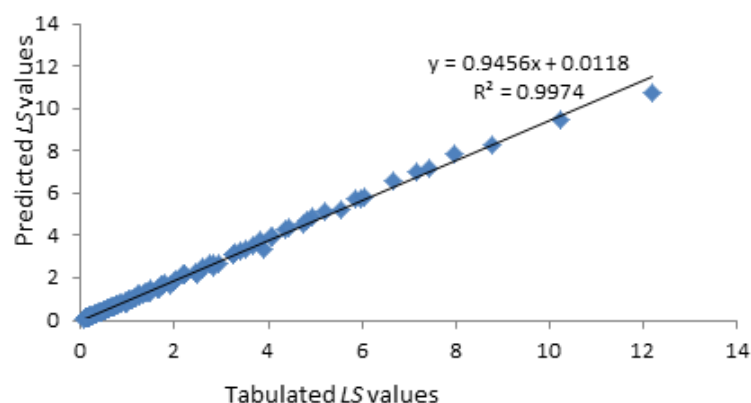


Figure 2: Correlation between the Predicted and Tabulated *LS* Values for Nabajuzi Watershed of Uganda

3.2. Erosion Risk Spots in Nabajuzi Watershed

Figure 3 shows the spatial patterns of soil erosion risk in Nabajuzi watershed. Soil erosion risk ranged from 0 to 125 t ha⁻¹yr⁻¹. These extreme cases were predicted in the valleys and in areas with bare soil or steep slope gradients, respectively. Soil erosion was described as nil (0 t ha⁻¹yr⁻¹), very low (1-5 t ha⁻¹yr⁻¹), low (6-10 t ha⁻¹yr⁻¹), moderate (11-20 t ha⁻¹yr⁻¹), high (21-40 t ha⁻¹yr⁻¹), and very high (41-125 t ha⁻¹yr⁻¹). With respect to the spatial pattern of erosion severity, all areas with high to very high erosion magnitude were considered as soil erosion hotspots in this watershed.

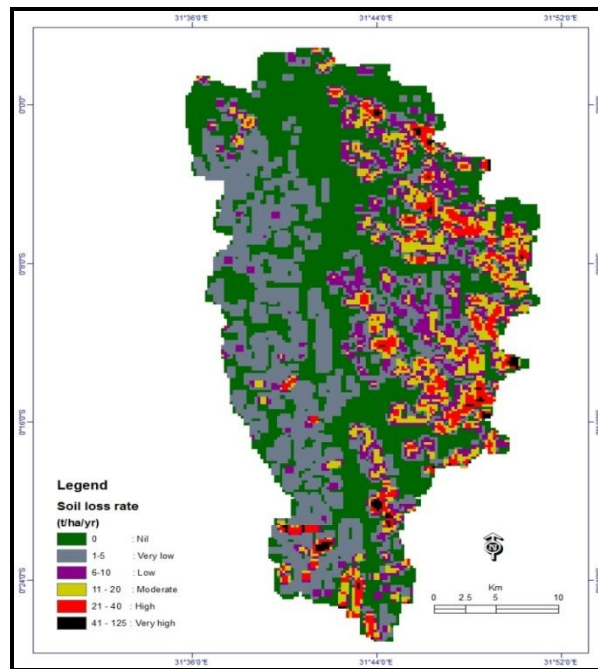


Figure 3: Spatial Pattern of Soil Erosion Risk in Nabajuzi Watershed in the LVB of Uganda

3.3. Variation of Erosion Risk with Landuse

The risk potential predicted for the different landuse is presented in Figure 4. This potential was highest in small scale farmland ($38 \text{ t ha}^{-1}\text{yr}^{-1}$), followed by built up area ($35 \text{ t ha}^{-1}\text{yr}^{-1}$), grassland ($24 \text{ t ha}^{-1}\text{yr}^{-1}$), woodland ($11 \text{ t ha}^{-1}\text{yr}^{-1}$), shrub land and seasonal wetland ($2.5 \text{ t ha}^{-1}\text{yr}^{-1}$) and lowest in permanent wetland ($0 \text{ t ha}^{-1}\text{yr}^{-1}$).

The high soil erosion risk potential in small scale farmland was expected as tillage destroys soil structure, making the soil highly susceptible to raindrop impact and runoff. This contradicts earlier findings by [8] and [21] who contended that a farmland can have less soil loss under proper management conditions. With regard to the Nabajuzi watershed, a common feature is that little ground cover management (mulches) coupled with the lack of physical structures for erosion control were originally identified as some of the most important concerns that underlain the high soil loss rates on cultivable land [40, 24].

The predicted soil erosion risk in the grassland, woodland, shrub land, seasonal and permanent wetlands were also expected and seemed to conform to the idea raised by [37] about the impact of vegetation in reducing runoff and soil loss. As canopy reduces raindrop impact, trees themselves also provide litter on the soil surface which decomposes to yield soil organic matter (SOM). This condition warrants soil aggregate stability towards runoff [26]; hence, generating moderately low erosion rates in these landuse as indicated in Figure 4. Besides, the roots bind the soil particles, increase macro pores in the soil, enhancing water infiltration, transpiring soil water and providing additional surface roughness by adding organic substances to the soil [39]. Plenty of literature indicates that grass cover is the most effective in reducing water erosion as compared to forest cover [4, 48, 5]. An unusual situation was recognized in the site whereby the grassland had more soil lost due to runoff as compared to the woodland area. A common practice is that in this watershed the grassland is usually degraded either through bush burning to regenerate pastures for animal grazing; or through cutting grasses to obtain residues for use as mulches in farms. This situation increases soil erosion particularly in the said landuse. On the other hand, the woodland in this site may have had a low soil loss rate compared to the grassland partly due to above ground cover as already discussed; or due to the root mechanical effect on soil strength as was previously claimed by [44]. The built up area had a

high soil loss rate because of existence of exposed soil surface in some parts, in addition to existence of concretized surfaces and roofs which increase the volume of runoff hence increasing soil loss most especially in the nearby highly susceptible soils.

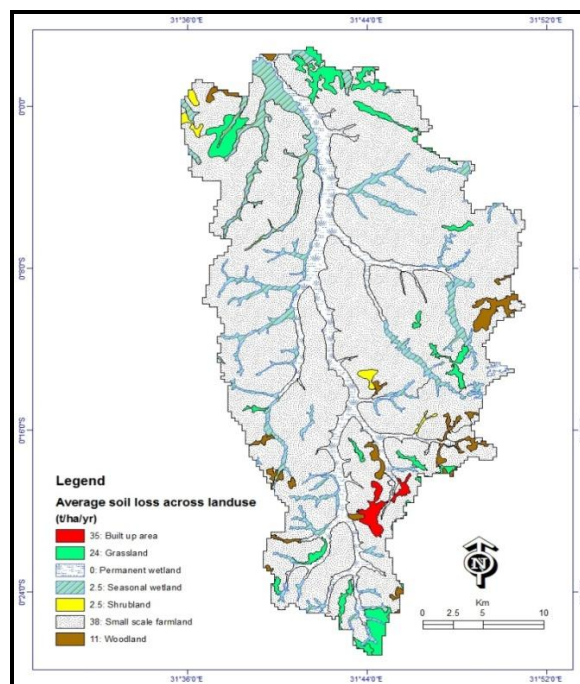


Figure 4: Variation of Soil Loss with Landuse Category in Nabajuzi Watershed in the LVB of Uganda

3.4. Variation of Erosion Risk with Soil Type

Figure 5 presents predicted erosion risk obtained in the various soil units. The risk was highest in Lixic Ferralsols ($50 \text{ t ha}^{-1}\text{yr}^{-1}$), followed by Acric Ferralsols ($20 \text{ t ha}^{-1}\text{yr}^{-1}$), Arenosols ($15 \text{ t ha}^{-1}\text{yr}^{-1}$), Gleyic Arenosols ($2.5 \text{ t ha}^{-1}\text{yr}^{-1}$) and Planosols ($0 \text{ t ha}^{-1}\text{yr}^{-1}$). The high erosion rates predicted in the Lixic Ferralsols and Acric Ferralsols were unexpected since these soil units are generally not impacted by erosion. Although such soils have high iron content, they are associated with low plant nutrients, a strong acidity and low available phosphorus. The existence of a high soil loss risk among them is most likely a manifestation of poor management as well as the effect of slope gradient on runoff and soil loss. On Arenosols, a moderate soil loss risk observed was expected since these soils are generally infertile and so, they are undisturbed by agricultural activities providing a less potential for soil loss to occur. Coupled with this, a greater portion of the Arenosols in Nabajuzi watershed is being covered by grassland which protects them against erosive agents. A very low or nil soil loss risk was noted on the Gleyic Arenosols and Planosols since these were soil units mapped in the wetland area with a high potential for deposition.

3.5. Relationship between Soil Erosion Risk and Slope Angle in Nabajuzi Watershed

According to a previous study conducted in the LVB [24], this area is greatly affected by rill and interrill erosion. Premised on this idea, three important arguments relating slope angle and soil loss rates can be discussed. First is that soil loss is a power function of percent slope gradient, with exponents ranging between 0.7 and 2.0 [46].

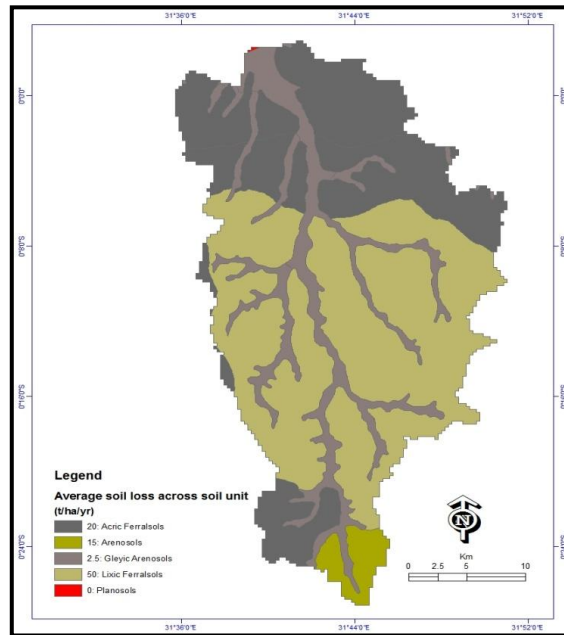


Figure 5: Variation of Soil Loss with Soil Type in Nabajuzi Watershed of LVB of Uganda

Second is that soil loss is a linear function of the sine of the slope gradient, with coefficients varying with slope gradient [27, 23]. Third is that soil loss is a polynomial function with the sine of slope gradient [45]. Yet, an earlier concern raised by [19] indicated that soil loss increases sharply with slope steepness until about 36%. But at steeper slopes which are greater than 86%, this curve relating slope steepness with soil loss rates flattens. Unfortunately, correlation coefficients to substantiate such claims at a watershed level are not readily available. In Nabajuzi watershed, slope percentages (Figure 6) were used to establish this coefficient of correlation between erosion risks and slope gradient. Potential erosion risk was highest (38–68) $t\ ha^{-1}yr^{-1}$ on the steepest slope gradient (15–18) %; and lowest (0–2.5) $t\ ha^{-1}yr^{-1}$ on the lowest slope gradient (0–5) %.

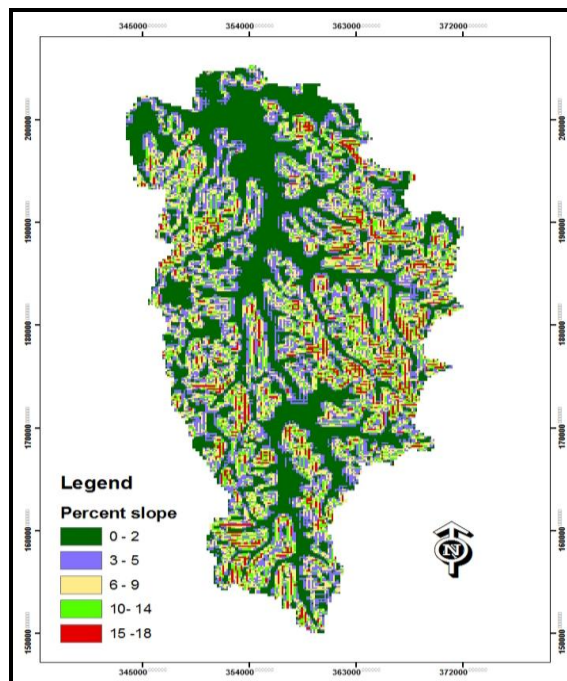


Figure 6: Slope Angle Categories in Nabajuzi Watershed of the LVB of Uganda

A strong linear relationship ($R= 0.96$) as in Figure 7, was recognized in this site; and soil erosion risk significantly varied with slope gradient ($P= 0.001$) at 95% significance level. This underscores the postulations by [19], [27] and by [23] as earlier discussed. Perhaps this observation is attributed to soil particle transport rather than to detachment processes; such that in absence of surface cover earlier highlighted by [40] for this watershed, runoff and soil loss increase with slope angle. A further empirical study investigating this issue is required in this watershed.

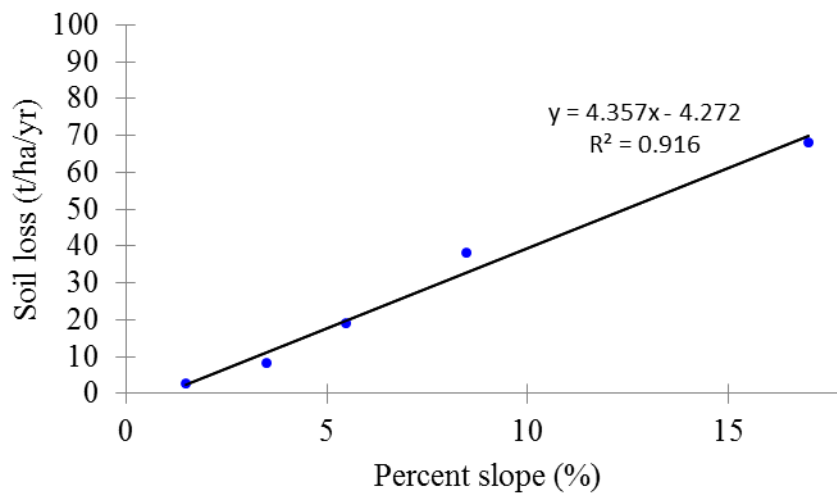


Figure 7: Correlating Slope Angle and Soil Loss in Nabajuzi Watershed in the LVB of Uganda

4. Conclusion

The predicted *LS* values derived by adapting RUSLE to C++ program had a strong linear correlation with the tabulated *LS* values. This C++ program expedites *LS* factor calculation particularly for a spatially heterogeneous watershed. This enables proper understanding of slope morphology and its related processes, thus fostering accurate erosion risk prediction at a large scale. Whereas the magnitude of erosion risk was generally moderate with respect to [11] rating, in some parts of Nabajuzi watershed a high risk potential was predicted. These areas require strategic maintenance for further reduction of soil erosion risk and restore the ecological functioning of Nabajuzi watershed of the LVB of Uganda.

Acknowledgement

We acknowledge research assistants and Sida Sarec (Swedish Research Grant) through Makerere University for partial funding.

References

- [1] Bagoora F.D.K., 1998: *Soil Loss in Rukiga Highlands in Eastern Kabale, Western Uganda*. Ph.D. Thesis, Makerere University, Kampala, Uganda.
- [2] Bamutaze Y., 2010: *Patterns of Water Erosion and Sediment Loading in Manafwa Catchment, Mt. Elgon, Eastern Uganda*. Ph.D. Thesis, Makerere University, Kampala, Uganda.
- [3] Bols P., 1978: *The Iso-erodent Map of Java and Madura*. Belgian Technical Assistance Project ATA 105, Soil Research Institute, Bogor.

- [4] De Baets S., Poesen J., Meersmans J. and Serlet L. *Cover Crops and Their Erosion-Reducing Effects during Concentrated Flow Erosion*. Catena. 2011. 85; 237-244.
- [5] De Baets S., Poesen J., Gyssels G., and Knapen A. *Effects of Grass Roots on the Erodibility of Top Soils during Concentrated Flow*. Geomorphology. 2006. 76; 54-67.
- [6] Desmet P. and Grovers G. *GIS-Based Simulation of Erosion and Deposition Patterns in an Agricultural Landscape: A Comparison of Model Results with Soil Map Information*. Catena. 1995. 25; 389-401.
- [7] Desmet P. and Grovers G. *A GIS Procedure for Automatically Calculating the USLE LS Factor on Topographically Complex Landscape Units*. Journal of Soil and Water Conservation 1996. 51 (5) 427-433.
- [8] Derpsch R. and Friedrich T., 2009: *Global Overview of Conservation Agriculture Adoption Proceedings*. Lead Paper, 4th World Congress on Conservation Agriculture, New Delhi, India. 429-438.
- [9] El-Hassanin A.S., Labib T.M. and Gaber E.I. *Effect of Vegetation Cover and Landscape on Runoff and Soil Losses from Watersheds of Burundi*. Agricultural Ecosystems and Environment. 1993. 43; 301-308.
- [10] El-Swaify S.A. *Factors Affecting Soil Erosion Hazards and Conservation Needs for Tropical Steep Lands*. Soil Technology. 1997. 11; 3-16.
- [11] Food and Agriculture Organization (FAO), 1990. FAO Yearbook 1989. Production, FAO Statistical Series No. 94, Vol. 43, FAO Rome, Italy.
- [12] Foster G.R., Lane L.J., Nowlin J.D., Laflen J.M. and Young R.A. *Estimating Erosion and Sediment from Field-Sized Area*. Transactions ASAE. 1981. 24; 1253-1262.
- [13] Griffin M.L., Beasley D.B, Fletcher J.J. and Foster G.R. *Estimating Soil Loss on Topographically Non-Uniform Field and Farm Units*. Journal of Soil and Water Conservation. 1988. 43; 326-331.
- [14] Ha N.T., 1996: *Definition of the Affected Factors to Soil Erosion and Prediction of Soil Loss in the Sloped Area*. Ph.D. Thesis, Hanoi University of Irrigation Science.
- [15] Halim R., Clemente R.S., Routray J. K. and Shrestha R.P. *Integration of Bio-Physical and Socio-Economic Factors to Assess Soil Erosion Hazard in the Upper Kaligarang Watershed, Indonesia*. Land Degradation and Development. 2007. 18; 453-469.
- [16] Harrop J.F., 1970: *The Soils of the Western Provinces of Uganda, Memoirs of the Research Division*. Series 1- Soils, No. 6, Department of Agriculture, Uganda.
- [17] Hickey R. Slope Angle and Slope Length Solutions for GIS. Cartography. 2000. 29 (1) 1-8.
- [18] Hickey R., Smith A. and Jankowski P. *Slope Length Calculations from a DEM within Arc/Info GRID*. Computers, Environment and Urban Systems. 1994. 18 (5) 365 - 380.
- [19] Horton R.E. *Erosional Development of Streams and their Drainage Basins: Hydrological Approach to Quantitative Morphology*. Geographical Society of America, Bulletin. 1945. 56; 275-370.

- [20] Hussein M.H. *An Analysis of Rainfall, Runoff and Erosion in the Low Rainfall Zone of Northern Iraq*. Journal of Hydrology. 1996. 181; 105-126.
- [21] Lal R. *Soil Science and Carbon Civilization*. Soil Science Society of America Journal. 2007. 71; 1425-1437.
- [22] Lillesand T.M. and Kiefer R.W., 1994: *Remote Sensing and Image Interpretation*. 3rd Ed., Wiley.
- [23] Liu B.Y., Nearing M.A. and Risse L.M. Slope Gradient Effects on Soil Loss for Steep Slopes. Transactions of America Society of Agriculture Engineers (ASAE). 1994. 37 (6) 1835-1840.
- [24] Lufafa A., Tenywa M.M., Isabirye M., Majaliwa M.J.G. and Woomeer P.L. *Prediction of Soil Erosion in a Lake Victoria Basin Catchment Using GIS-Based USLE Model*. Agricultural Systems. 2003. 76 (3) 883-894.
- [25] Majaliwa M.G.J., 2005: Soil Erosion from Major Agricultural Landuse types and Associated Pollution Loading in Selected Lake Victoria Micro-Catchments. Ph.D. Thesis, Makerere University, Kampala, Uganda.
- [26] Mamo M. and Bubbenzer G.D. *Detachment Rate, Soil Erodibility and Soil Strength as Influenced by Plant Roots: Laboratory and Field Study (Part 1 and 2)*. Transactions of American Society of Agricultural Engineers. 2001. 44; 1167-1187.
- [27] McCool D.K., Brown L.C., Foster G.R., Mutchler C.K. and Meyer L.D. *Revised Slope Steepness Factor for the Universal Soil Loss Equation (USLE)*. Transactions of America Society of Agriculture Engineers (ASAE). 1987. 30 (5) 1387-1396.
- [28] Mitasova H. *Surfaces and Modeling*. Grass Clippings. 1993. 7 (1) 18-19.
- [29] Mitasova H., Hofierka J., Zlocha M. and Iverson L. *Modeling Topographic Potential for Erosion and Deposition using GIS*. International Journal of GIS. 1996. 10 (5) 629-641.
- [30] Moore R.R. *Rainfall Erosivity in East Africa: Kenya, Tanzania and Uganda*. Geografika Annaler. Series A. Physical Geography. 1979. 61; 147-156.
- [31] Moore I.D. and Wilson J.P. *Length-Slope Factors for the Revised Universal Soil Loss Equation (RUSLE): Simplified Method of Estimation*. Journal of Soil and Water Conservation. 1992. 47 (5) 423-428.
- [32] NRCS-USDA, 2002: *Technical Guide to RUSLE use in Michigan, State Office of Michigan*. Institute of Water Research, Michigan State University. www.iwr.msu.edu/rusle/lstable.htm.
- [33] Renard K.G., Foster G.R., Weesies G.A., McCool D.K., and Yoder D.C., 1997. *Predicting Soil Erosion by Water: Guide to Conservation Planning with the Revised Universal Soil Loss Equation (RUSLE)*. Agricultural Hand Book, Vol. 703. US Department of Agriculture, Washington, DC, USA. 1-251.
- [34] Renard K., G.R. Foster, G.A. Weesies and J.P. Porter. *RUSLE Revised Universal Soil Loss Equation*. Journal of Soil and Water Conservation. 1991. 46; 30-33.

- [35] Renschler C.S. and Harbor J. *Soil Erosion Assessment Tools from Point to Regional Scales-the Role of Geomorphologists in Land Management Research and Implementation*. *Geomorphology* 2002. 47; 189-209.
- [36] Shi Z.H., Cai C.F., Ding S.W., Wang T.W., and Chow T.L. *Soil Conservation Planning at Small Watershed Level Using RUSLE with GIS: A Case Study In Three Gorge Area of China*. *Catena*. 2004. 55; 33-48.
- [37] Sinun W., Wong W.M., Douglas I. and Spencer T., 1992: *Through Fall, Stem Flow, Overland Flow and Through Flow in the Ulu Segaman Rain Forest, Sabah*. *Phil. Transactions of the Royal Society, London, UK*, B335-389-395.
- [38] Srinivasan R. and Engel B.A. *Effect of Slope Prediction Methods on Slope and Erosion Estimates*. *Applied Engineering in Agriculture*. 1991. 76 (6) 779-783.
- [39] Styczen M.E. and Morgan R.P.C., 1995: *Engineering Properties of Vegetation*. In: Morgan, R.P. C., Rickson, R.J., Eds. *Slope Stabilization and Erosion Control: A Bioengineering Approach*: E and F.N. Spon, London, 5-58.
- [40] Tenywa M.M., Isabirye M.I., Lal R., Lufafa A., and Achan P. *Cultural Practices and Production Constraints in Smallholder Banana-Based Cropping of Uganda's Lake Victoria Basin*. *African Crop Science Journal*. 1999. 7 (4) 541-550.
- [41] Van Remortel R., Maichle R. and Hickey R. *Computing the RUSLE LS Factor Based on Array-Based Slope Length Processing of Digital Elevation Data Using a C++ Executable*. *Computers and Geosciences*. 2004. 30 (9/10) 1043-1053.
- [42] Wischmeier W.H. and Smith D.D., 1965: *Predicting Rainfall Erosion Losses from Crop Land East of the Rocky Mountains: A Guide for Selection of Practices for Soil and Water Conservation*. Agriculture, Washington, DC, USA.
- [43] Wischmeier W.H. and Smith D.D., 1978: *Predicting Rainfall Erosion Losses*. US Department of Agriculture (USDA), Agricultural Research Service, Hand Book No. 537, 58.
- [44] Wu W.D., Zheng S.Z. and Lu Z.H. *Effect of Plant Roots on Penetrability and Anti-Scourability of Red Soil Derived from Granite*. *Pedosphere*. 2000. 10; 183-188.
- [45] Zhang K.L. and Hosoyamada K. *Influence of Slope Gradient on Interrill Erosion of Shirasu Soil*. *Soil Physical Conditions and Plant Growth in Japan*. 1996. 73; 37-44.
- [46] Zhang X.C., Nearing M.A., Miller M.P., Norton L. and West L.T. *Modelling Interrill Sediment Delivery*. *Soil Science Society of America Journal*. 1998. 62 (2) 438-444.
- [47] Zhang H., Yang Q., Li R., Liu Q., Moore D., He P., Ritsema C. J., and Geissen V. *Extension of a GIS Procedure for Calculating the RUSLE Equation LS Factor*. *Computers and Geosciences*. 2013. 52; 177-188.
- [48] Zhou Z.C. and Shangguan Z.P. *The Effects of Ryegrass Roots and Shoots on Loess Erosion under Simulated Rainfall*. *Catena*. 2007. 70; 350-355.